Proceedings of the 10th World Congress on Civil, Structural, and Environmental Engineering (CSEE 2025)
Barcelona, Spain - April, 2025
Paper No. ICGRE 157
DOI: 10.11159/icgre25.157

Prediction of Active Earth Pressure in Constrained Backfill Retaining Walls using Non-Linear Regression and SVR

S Danish Bashir[1], Abdul Waris Kenue[1], B Munwar Basha[1]
[1]Department of Civil Engineering, Indian Institute of Technology Hyderabad
Hyderabad, India – 502285
ce22resch11002@iith.ac.in, ce22resch11001@iith.ac.in, basha@ce.iith.ac.in

Abstract: Constrained Backfill Retaining Walls (CBRWs) are increasingly utilized in geotechnical engineering, particularly in mountainous regions and densely populated urban areas where space limitations demand innovative design solutions. These walls exhibit unique geometric configurations, leading to complex earth pressure behaviors that deviate significantly from those observed in conventional retaining walls. Accurate prediction of the coefficient of active earth pressure (K_a) is crucial for ensuring the stability and safety of CBRWs. However, traditional methods using data-fitting software, though often yielding high R^2 values (up to 0.99), may not provide reliable predictions in real-world applications. To address these shortcomings, this study investigates the application of machine learning (ML) techniques, specifically Support Vector Regression (SVR), as an advanced method for predicting K_a in CBRWs. The current investigation models three failure mechanisms involving single, double, and triple rigid blocks, depending on the distance between the rock face and the retaining wall, to generate a dataset of K_a, calculated through in-house MATLAB codes. These computations are both time-consuming and computationally intensive, highlighting the necessity for an efficient predictive model. The SVR model is employed to predict K_a, and its performance is compared against conventional data-fitting approaches. The input parameters for the predictions include – aspect ratio (b/h), internal frictional angle of the soil (ϕ), rock-face angle (η), retaining wall inclination (β), backfill inclination (ε), interface friction angle between rock-face and soil (δ), and interface friction angle between retaining wall and soil (ψ). The model effectiveness is evaluated using multiple error metrics. The SVR model achieved a coefficient of determination (R^2) value of 97.4%, demonstrating strong predictive capability. In contrast, conventional data-fitting software exhibits limitations in accurately capturing the complex K_a behavior in CBRWs. The findings of this study underscore the potential of SVR to enhance the design and analysis of CBRWs by offering greater accuracy and computational efficiency compared to traditional methods.
Keywords: Constrained backfill, Retaining walls, Support Vector Regression, Multi-wedge failure, Earth Pressure.

1. Introduction

Constrained backfill retaining walls (CBRWs) have emerged as indispensable structures in geotechnical engineering, particularly in scenarios where space limitations pose significant challenges. These walls are commonly employed in mountainous terrains and densely populated urban regions, where the availability of land for conventional retaining wall designs is restricted. Unlike traditional retaining walls that rely on semi-infinite backfill for stability, which leads to a linear distribution of active earth pressure and a single triangular failure wedge as shown in Fig. 1(a). These assumptions are unsuitable for CBRWs (Yang and Tang 2017), where the proximity of the rock face or other boundary constraints significantly alters the failure mechanisms. CBRWs feature limited backfill widths, necessitating specialized design considerations to account for their unique geometric and structural characteristics. The constrained backfill geometry of CBRWs introduces complexities in the behaviour of earth pressure as shown in Fig. 1(b), making the prediction of the coefficient of active earth pressure (K_a) a critical aspect of their design. The proximity of a rock face or other boundary conditions significantly affects the distribution and magnitude of active earth pressures, deviating from the assumptions of classical theories such as Rankine (1857) and Coulomb (1776). These variations have direct implications for the stability, safety, and cost-effectiveness of retaining wall structures, underscoring the importance of accurate analytical and predictive models (Chen et al. 2017). The narrow backfill geometry in CBRWs results in multiple failure wedges and a non-linear pressure distribution, which classical methods cannot accommodate (Ahmed and Basha 2021). Additionally, traditional approaches often neglect critical factors such as the interaction between the retaining wall and the rock face (Xu et al. 2022), the influence of varying interface friction angles, and the impact of wall inclinations or backfill slopes. Consequently, advancing the understanding of their behaviour and developing reliable predictive tools are essential to ensure their optimal performance and long-term sustainability.

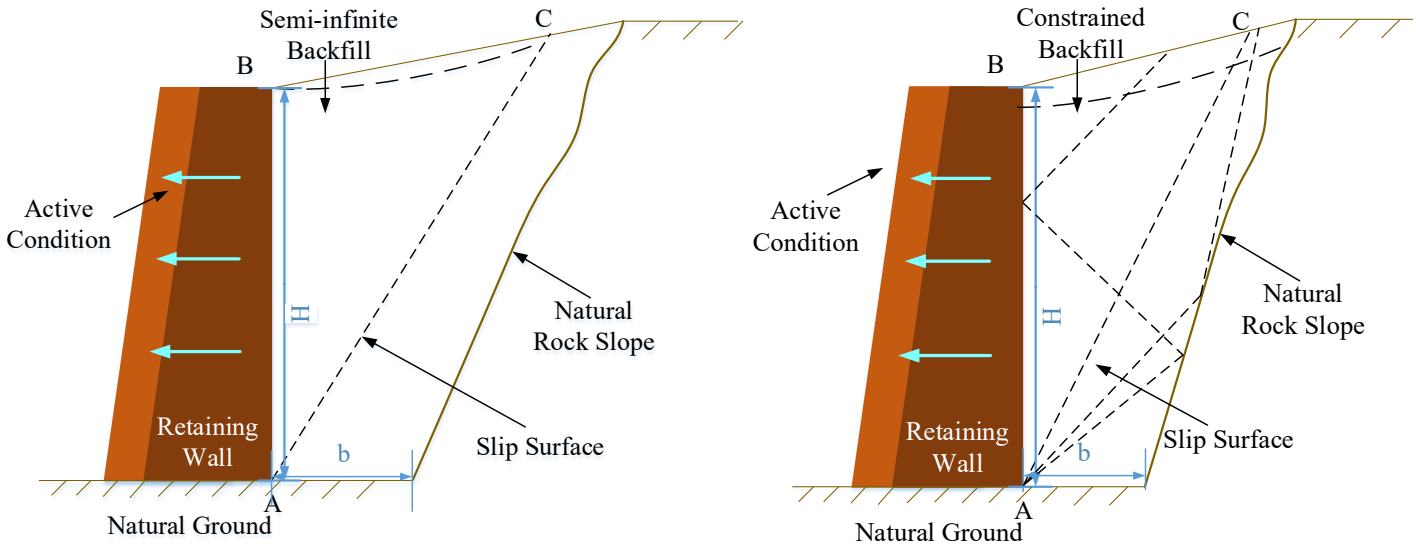

(a) Conventional Retaining walls (b) Constrained Backfill retaining Walls

Fig. 1: Retaining walls with (a) Semi-infinite backfill, and (b) Constrained backfill.

In recent years, geotechnical engineering has witnessed the increasing adoption of artificial intelligence, machine learning (ML), and soft computing models as indispensable tools for addressing complex challenges in subsurface analysis and design (Mahmoodzadeh et al., 2022; Waris et al., 2024). Conventional data-fitting tools, though capable of producing high R^2 values, often fail to generalize and lack the ability to provide insights into the underlying physics of the problem, limiting their practical applicability in varied scenarios. ML-based predictive models have emerged as powerful alternatives to traditional approaches. These models excel in capturing the intricate and nonlinear behaviours inherent in complex systems, enabling accurate representations of active earth pressure in CBRWs. Unlike traditional methods, ML techniques such as Support Vector Regression (SVR) bypass restrictive assumptions, offering robust, efficient, and generalizable predictions. Recently, Waris et al. (2024) highlighted that meeting performance metrics alone does not guarantee that an AI/ML model captures the underlying physics of a phenomenon. To address this concern, they emphasized the use of domain-based error validation models that go beyond merely achieving goodness-of-fit criteria.

1.1 Objectives

This study aims to address the limitations of traditional regression methods in predicting K_a in CBRWs by employing advanced predictive models. The specific objectives include:

1. Highlighting the shortcomings of classical theories and data-fitting approaches in capturing the non-linear and complex earth pressure behaviour of CBRWs.
2. Development of a robust and efficient predictive model using ML, specifically SVR, capable of accurately modelling the K_a.
3. Comparison of the performance of SVR model with traditional data-fitting tools using multiple error metrics, highlighting its superiority in terms of accuracy and reliability.
4. Illustrate the potential of ML in solving complex geotechnical problems, paving way for broader applications in geotechnical engineering.

2. Methodology

The dataset for this study is generated by implementing the methodology proposed by Ahmed and Basha (2021), which employed the multi-wedge theory for calculating K_a in retaining walls with constrained backfills. This approach considers the reflective shear zones between the wall and the rock face and incorporates three distinct failure mechanisms for a comprehensive evaluation.

2.1 Multi-wedge failure mechanism

The analytical model involves three wedge failure mechanisms to simulate active earth pressure acting on retaining walls.

Mechanism-1 (Single Block Failure) involves a single block with a straight-line failure surface passing through the heel of the retaining wall. Mechanism-2 (Two-Block Failure) comprises of two blocks in the active wedge, one triangular and another trapezoidal block. Lastly, Mechanism-3 (Three-Block Failure) includes three blocks – two trapezoidal blocks

and one triangular block. Each block is defined by slip planes inclined at specific angles relative to the horizontal. These angles are optimized by employing a multi-dimensional improved Nelder–Mead simplex routine to maximize active thrust. These mechanisms are depicted in Fig. 2. For cases where the rock face is sufficiently distant, such that $b/h \geq 0.7$, the failure wedge forms a triangular shape. When the backfill width is reduced to $0.3 \leq b/h \leq 0.6$, the failure mechanism evolves into two wedges: a triangle and a trapezoid. A further reduction in backfill width ($b/h \leq 0.3$) results in three distinct wedges comprising a triangle and two trapezoids.

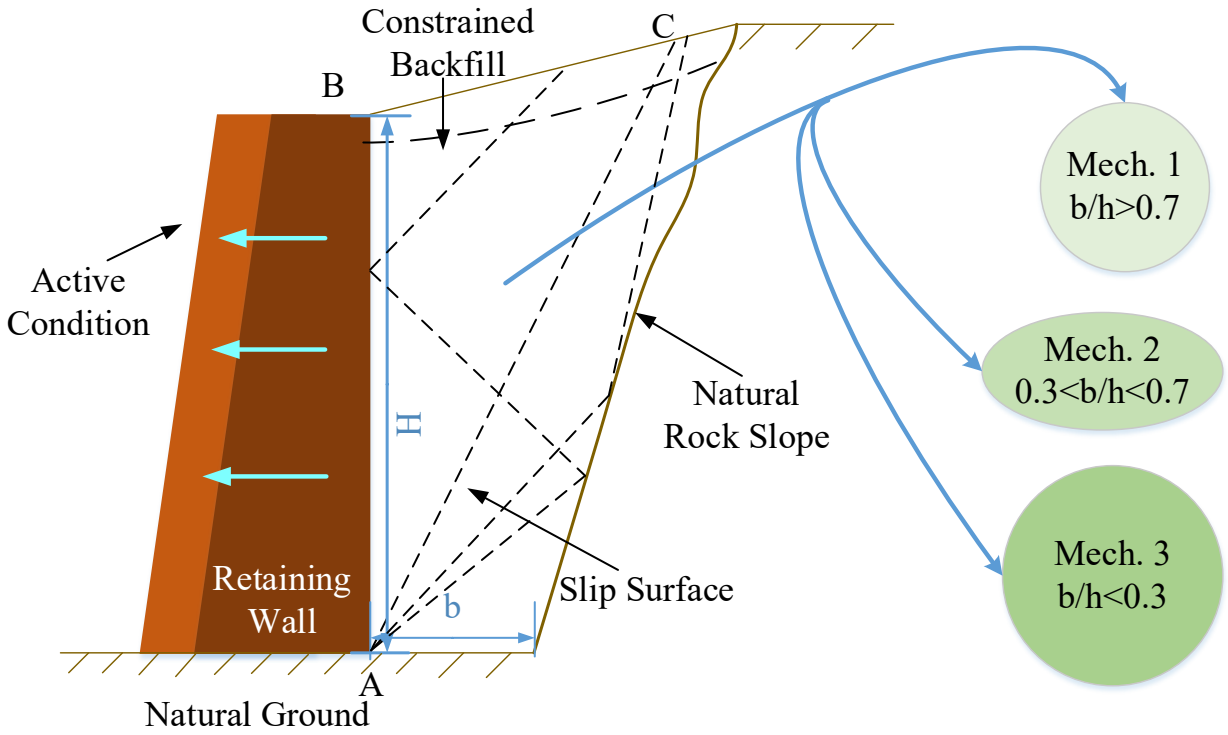

Fig. 2: Three wedge failure mechanism as proposed by Ahmed and Basha (2021).

2.3 Dataset Generation

Data serves as the cornerstone of ML, with its quality, quantity, and relevance significantly influencing the success of predictive models. Ahmed and Basha (2021) conducted an extensive analytical investigation, offering mathematical formulations to create a robust database using advanced coding techniques. A dataset comprising 12,006 data points is generated to facilitate the training of the various ML models. Table 1 provides a detailed statistical overview of the input parameters.

Table 1. Statistical information of the input and output variables in the dataset

	φ_r	β	ε	η	δ_p	ψ_P	δ_r	ψ_r	b/h	K_a
Total data points	12006	12006	12006	12006	12006	12006	12006	12006	12006	12006
Arithmetic mean	33.77	100.07	4.98	79.94	22.43	22.48	16.83	16.87	0.79	0.39
Standard deviation	7.39	8.15	4.08	8.15	16.77	16.77	13.40	13.40	0.49	0.12
Minimum	25.00	90.00	0.00	70.00	0.00	0.00	0.00	0.00	0.10	0.11
Maximum	45.00	110.00	10.00	90.00	45.00	45.00	45.00	45.00	1.50	1.44

To establish a baseline for predicting K_a, a traditional data-fitting technique is also employed. This approach involves fitting a non-linear model to the dataset generated using Datafit software, and the model's performance is evaluated using various statistical metrics. The model performance shows a very low explanatory power, as indicated by the coefficient of determination (R^2) of 0.17% and the adjusted R^2 of 0.098%, suggesting that the model is unable to fit the data. The residual analysis reveals significant discrepancies between the predicted and observed values, with a sum of residuals of 3,594,126 and an average residual of 297.6. The residual sum of squares, both absolute and relative, is extremely high

(5.05×10^{63}), further emphasizing the model's poor fit. The standard error of the estimate is 2.05×10^{16}, indicating large errors in predictions. Additionally, the proportion of variance explained is only 0.173%, which reinforces the limited predictive capability of the model. However, the Durbin-Watson statistic of 2.0026 suggests that there is no significant autocorrelation in the residuals, meaning the residuals are independent of each other. These results clearly demonstrate that the model is fundamentally flawed, offering no reliable predictions. The performance metrics are abysmal, indicating that the model fails miserably in capturing the underlying patterns in the data. It is evident that this model is unsuitable and needs to be completely discarded, as it does not provide any meaningful or accurate results.

2.4 Support Vector Regression

Vapnik (1995) introduced the support vector machines (SVM) technique, which serves as the foundation for the extension to SVR. This extension of SVMs caters specifically to regression (Guardiani et al. 2022). Importantly, SVM is designed for categorical target variables, whereas SVR is better suited for continuous target variables. It is worth noting that SVR is a non-parametric method due to its reliance on kernel functions. The SVR algorithm endeavors to identify a hyperplane that optimally accommodates the data points within a continuous space while minimizing prediction errors (identifying the narrowest tube) (Sethi, 2020). Mathematically, the regression function is defined as:

$$K_a(\mathbf{x}) = \mathbf{w}^T \varpi(\mathbf{x}) + b$$

where,

$$\mathbf{x} = \left[b/h,\ \phi,\ \eta,\ \beta,\ \varepsilon,\ \delta,\ \psi \right] \tag{1}$$

The key components in the context of the above equation are the non-linear mapping function ϖ, the training set $\{(x_1, (K_a)_1), (x_2, (K_a)_2), \ldots, (x_m, (K_a)_m)\}$, input features or the factors x_i contributing to the output label or K_a, weight vector $\boldsymbol{w}$, and offset from the hyperplane's origin b are key components in the context of the equation. The determination of these parameters involves minimizing an objective function while adhering to specific constraints. The objective of these constraints is to restrict the discrepancy between the predicted output and the actual measured output within a predefined threshold value ν. In order to accommodate certain data points lying outside the ν-tube, a soft margin approach is employed, which introduces slack variables, ξ (Guardiani et al. 2022). The convex objective function, can be expressed as follows (Bermolen 2009):

$$\min_{w,b,\xi,\xi^*} \left(\frac{1}{2} \mathbf{w}^T \mathbf{w} + C \sum_{i=1}^{m} \left(\xi_i + \xi_i^* \right) \right)$$

$$\text{subject to } \begin{cases} \left(K_a\right)_i - \mathbf{w}^T \varpi(\mathbf{x}_i) - b \le \nu + \xi_i, \\ \mathbf{w}^T \varpi(\mathbf{x}_i) + b - \left(K_a\right)_i \le \nu + \xi_i^*, \\ \xi_i, \xi_i^* \ge 0, i = 1, \ldots, n \end{cases} \tag{2}$$

To ensure accurate fitting, a convex loss function is initially established. The primary objective is to minimize this function, thereby identifying the flattest tube that encompasses a significant portion of the training samples. The function $K_a(\mathbf{x})$ can also exhibit non-linearity, it is then possible to map the data into a higher-dimensional space known as the kernel space. Within this transformed space, all the data points can be effectively separated in a linear manner. In the case of nonlinear regression problems, the decision function from the dual problem can be expressed as follows [Lin et al., 2021]:

$$K_a(\mathbf{x}) = \sum_{i=1}^{m} \left(\alpha_i - \alpha_i^* \right) k(\mathbf{x}, \mathbf{x}_i) + b \tag{3}$$

where, α, α^* are the Lagrange multiplier, k ($\mathbf{x}$, $\mathbf{x}_i$) are the kernel function. The ML model is to be tuned for the best kernel function. The model parameters, such as the penalty parameter (c), kernel coefficient (γ), and threshold (ν), are optimized using a grid search with cross-validation to avoid overfitting and enhance generalizability.

The dataset is divided into training and testing subsets, ensuring an 80:20 split. Five-fold cross-validation is employed during training to evaluate the model's performance and stability. Key metrics, including R^2, mean squared error (*MSE*), and mean absolute error (*MAE*), are used to assess the model's predictive accuracy.

3. Results and Discussion

3.1 Performance Evaluation

The SVR model demonstrates exceptional predictive accuracy, with R^2 values of 97.4%, 97.2%, and 96.5% for training, cross-validation, and testing phases, respectively. These metrics highlight the model's ability to maintain consistency and reliability across different data splits. Furthermore, the SVR model achieves a low *MSE* of 0.033 and an *MAE* of 0.065, underscoring its capacity to capture complex interactions between the input parameters and active earth pressure with precision.

In stark contrast, the traditional data-fitting method exhibits a negligible R^2 value, indicating an almost complete failure to explain the variance in the dataset. Additionally, the method's excessively high residuals, reveal significant inaccuracies and limitations. These results clearly highlight the inadequacy of the traditional data-fitting approach and emphasize the superiority of the SVR model as a robust and reliable predictive framework for constrained backfill retaining walls.

3.2 Prediction of the active earth pressure coefficient using SVR

The K_a values are calculated using MATLAB based on complicated formulations, as well as predicted through an SVR model trained on the generated dataset. The prediction accuracy of the SVR model is assessed by error metrics summarized in **Table 2**. The results demonstrate that the SVR model consistently provides highly accurate predictions of K_a, with an R^2 value exceeding 95%, indicating a strong correlation between the predicted and actual values. The *MAE* highlights the average magnitude of prediction errors, showing that the discrepancies between the predicted and actual values are minimal. The low *MSE*, which penalizes larger deviations more heavily, confirms that significant errors are rare and that the model provides consistent accuracy across the dataset.

Table 2: Standard metrics of SVR

Metric		Value
R^2	Train	97.4%
	CV	97.2%
	Test	96.5%
MAE		0.065
MSE		0.033

3.3 Comparison of Actual and Predicted Values

Figure 3 presents the scatter plot of the actual versus predicted values of the K_a obtained using the SVR model. Each data point represents a pair of actual and predicted values. The 45° reference line in the plot corresponds to an ideal scenario where the predicted values perfectly match the actual ones. The data points in the scatter plot are closely aligned along this diagonal line, demonstrating that the SVR model provides highly accurate predictions. Minimal deviation from the line indicates that the model effectively captures the underlying trends in the dataset and predicts K_a values with high precision.

Moreover, the alignment of points across the entire range of K_a values shows that the model performs consistently, regardless of the magnitude of K_a. This result highlights the robustness of the SVR model in predicting K_a across diverse input conditions, as reflected in the high R^2 value reported in **Table 2**. The performance of the SVR model can be attributed to its ability to model non-linear relationships between input parameters and K_a. This capability allows the model to generalize well, even for complex conditions, and ensures that predicted values remain close to their actual counterparts.

3.4 Density Plot

Figure 4 presents a density plot of the K_a values, complemented by an inset error histogram to provide a detailed understanding of the data distribution and prediction accuracy of the SVR model. The density plot highlights the distribution of K_a values across the dataset. The density plot highlights the distribution of K_a values across the dataset. A prominent peak is observed, indicating that a majority of the data points fall within a tolerable error range. The inset error histogram depicts the distribution of prediction errors, calculated as the difference between the actual and predicted K_a values. The histogram is centred around zero, signifying that the SVR model produces unbiased predictions with no systematic overestimation or underestimation of K_a. The symmetrical shape of the histogram indicates that the errors are evenly distributed, with most errors being small in magnitude. This observation is further supported by the low frequency

of errors in the tails, demonstrating that significant deviations are rare. Together, the density plot and the error histogram illustrate the SVR model's high accuracy and consistency in predicting K_a. The combination of these visualizations provides a comprehensive analysis of the model's performance, highlighting its capability to generalize effectively across diverse input conditions while maintaining minimal prediction errors.

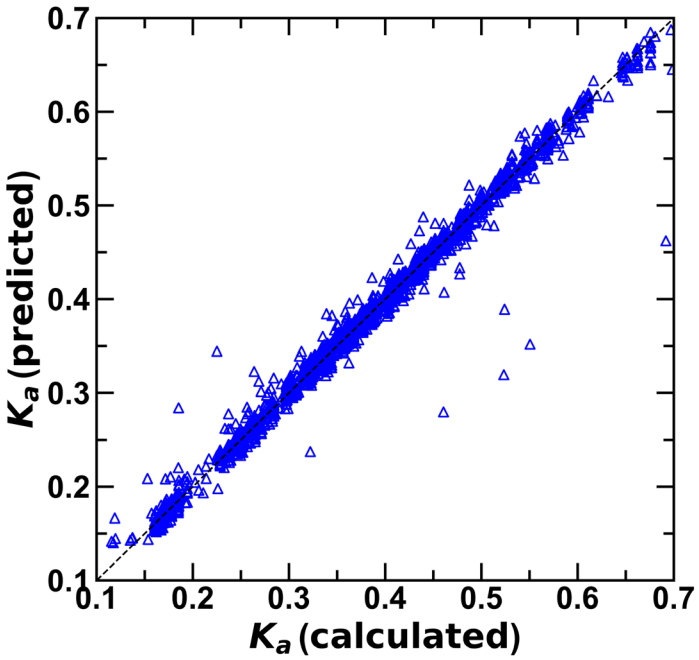

Fig. 3: Scatter plot comparing the actual and the predicted values of K_a using SVR model.

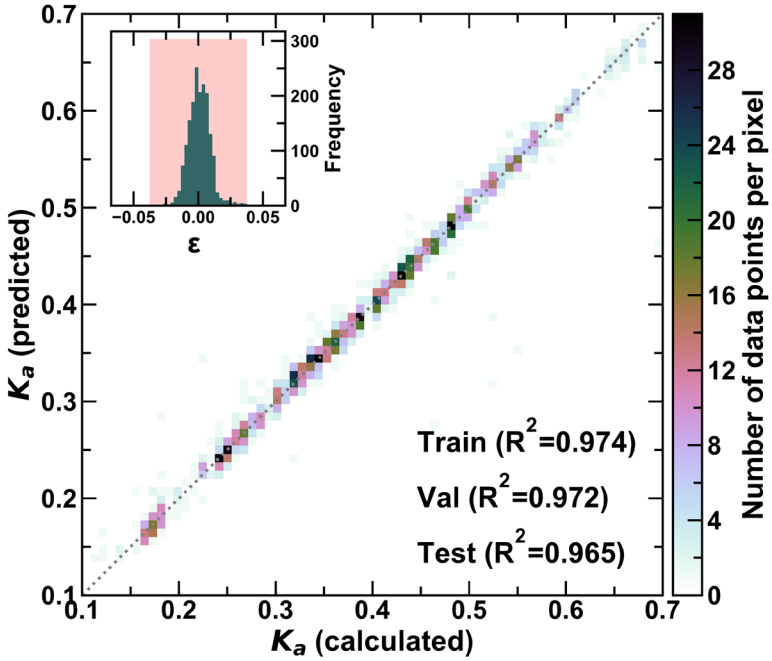

Fig. 4: Density plot and the inset error histogram of SVR.

domain-based error validation is adopted in the current study. **Fig. 5** depicts a significant decrease in the K_a as the aspect ratio (b/h) decreases from 0.7 to 0.1, across various friction angles. This reduction is attributed to the partial development of failure planes caused by the constraint imposed by the rock face boundary. Notably, for ϕ = 42° and ϕ = 45°, the model predicts values that closely align with calculated values, indicating high accuracy, particularly at higher friction angles. Also, when b/h falls between 0.3 to 0.6, the model exhibits higher accuracy for all ϕ values, with minimal

errors observed. However, at ϕ = 28°, the predicted value of k_a is 11% higher than the calculated value when the b/h ratio is 0.2. Similarly, for ϕ = 32° and ϕ = 36°, the observed errors between the predicted and calculated values of K_a are 10% and 7.7%, respectively at b/h = 0.2. It is essential to acknowledge that the inherent complexity involved in computations considering more mechanisms limits the availability of data points for lower aspect ratios (b/h < 0.3). This scarcity of data is manifested in the model's observed errors. Expanding the dataset by augmenting the number of data points for b/h ratios below 0.3 presents a viable approach to mitigate this limitation and enhance the model's accuracy. Moreover, at b/h = 1.0, the errors between predicted and calculated values of k_a are 5% for ϕ = 28°, 4.5% for ϕ = 32°, and 4% for ϕ = 36°. The findings suggest that the model effectively predicts K_a values across various aspect ratios and friction angles. However, they also emphasize the necessity for additional data generation, particularly for lower aspect ratios, to further improve the accuracy of the model.

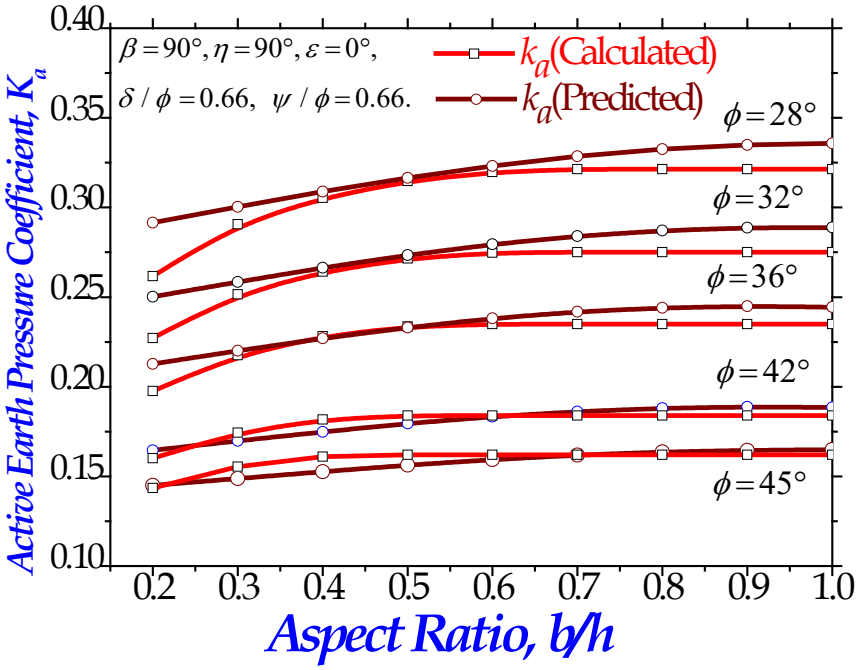

Fig. 5: Effect of ϕ and b/h on K_a

3.5 Practical Implications

The enhanced predictive accuracy of the SVR model offers significant practical benefits for the design of CBRWs. By providing reliable predictions of active earth pressure, the model enables more precise and efficient structural designs, reducing the risk of overdesign or structural failure. This methodological advancement underscores the potential of machine learning to transform geotechnical engineering practices, particularly for complex applications like CBRWs, where traditional methods fall short.

4 Conclusions

This study aims to develop an ML model for estimating the K_a or constrained backfill width retaining walls operating under translation mode. A dataset of 12,006 K_a values is generated through limit equilibrium analysis of CBRWs. This study demonstrates the superior predictive capability of the SVR model in estimating active earth pressure for CBRWs. With R^2 values of 97.4%, 97.2%, and 96.5% for training, cross-validation, and testing datasets, the SVR model consistently outperforms traditional data-fitting techniques, which fail to provide meaningful results (R^2 = 0.17%). The SVR model also exhibits minimal prediction error, as reflected by *MSE* of 0.033 and a mean absolute error of 0.065. In contrast, traditional methods are shown to be unsuitable for handling the complexities of narrow backfill geometries and boundary constraints. The errors between predicted and calculated values of K_a are 11% for ϕ = 28°, 10% for ϕ = 32°, and 7.7% for ϕ = 36° when the b/h ratio is 0.2. Moreover, at b/h = 1.0, the errors are 5% for ϕ = 28°, 4.5% for ϕ = 32°, and 4% for ϕ = 36°.

References

[1] S. M. Ahmed, B. M. Basha, "External Stability Analysis of Narrow Backfilled Gravity Retaining Walls," in *Geotech Geol Eng* 39, 1603–1620, 2021. https://doi.org/10.1007/s10706-020-01580-3

[2] P. Bermolen and R. Dario, "Support vector regression for link load prediction." *Computer Networks* 53, no. 2, 191-201, 2009. https://doi.org/10.1016/j.comnet.2008.09.018

[3] J. J. Chen, M. G. Li and J. H. Wang, "Active earth pressure against rigid retaining walls subjected to confined cohesionless soil," *Int J Geomech* 17(6):06016041, 2017. https://doi.org/10.1061/(ASCE)GM.1943-5622.0000855

[4] C. A. Coulomb, "Essais sur une application des regles des maximis et minimis a quelques problems de statique relatits a l'architecture," *Mem. Acad. Roy. Sci. Pres. Sav*., Paris, 7, 343-382, 1776.

[5] C. Guardiani, E. Soranzo, and W. Wu, "Time-dependent reliability analysis of unsaturated slopes under rapid drawdown with intelligent surrogate models," *Acta Geotech* 17, 1071–1096, 2022. https://doi.org/10.1007/s11440-021-01364-w

[6] A. Mahmoodzadeh, M. Mohammadi, H. F. M. Ali, H. H. Ibrahim, S. N. Abdulhamid and H. R. Nejati, "Prediction of safety factors for slope stability: comparison of machine learning techniques," *Nat Hazards* 111(2):1771–1799,2022. https://doi.org/10.1007/s11069-021-05115-8

[7] W. J. M. Rankine, "On the stability of loose earth'" Phil. Trans. R. Soc. 147, 9–27, 1857.

[8] A. Sethi, "Support Vector Regression Tutorial for Machine Learning." *Analytics Vidhya.* Retrieved June 15, 2023, from https://www.analyticsvidhya.com/blog/2020/03/support-vector-regression-tutorial-for-machine-learning/

[9] V. N. Vapnik, "The nature of statistical learning theory." Springer, New York, 1995.

[10] K. A. Waris, S. J. Fayaz, A. H. Reddy, B. M. Basha,. "Pseudo-static slope stability analysis using explainable machine learning techniques." *Nat Hazards* (2024). https://doi.org/10.1007/s11069-024-06839-z

[11] L. Xu, H. Chen, FQ Chen, Y. Lin, and C. Lin, "An experimental study of the active failure mechanism of narrow backfills installed behind rigid retaining walls conducted using Geo-PIV." *Acta Geotechnica* 17, 9:4051-4068, 2022. https://doi.org/10.1007/s11440-021-01438-9

[12] K. H. Yang, J. Ching and J. G. Zornberg, "Reliability-based design for external stability of narrow mechanically stabilized earth walls: calibration from centrifuge tests," *J. Geotech. Geoenviron. Eng*. 137 (3), 239–253, 2011. https://doi.org/10.1061/(ASCE)GT.1943-5606.0000423